FTAS/TR-66-13

APPARATUS FOR THE INVESTIGATION OF INSTABILITIES

IN GAS COOLED HEAT EXCHANGER TUBES

by

Edward R. Kolbe

November 1966

ABSTRACT

Steady-state gas flow characteristics in slender heated tubes indicate that for a given pressure drop, a unique flow rate does not exist. Of the two or possibly three flow rates, the one having a negative rate of change of pressure drop with flow rate at constant heat input is unstable. For gases this condition usually occurs when the flow in the tube is laminar . Details of the design, construction, and initial tests of apparatus for the investigation of the "laminar instability" problem are presented in this report. Results of previous work on both the steady-state and dynamical problem are discussed and used in the prediction of experimental results for helium in an electrically-heated .094" ID x 54" tube.

For a gas cooled passage it is indicated that there are only two flow rates for a given pressure drop and heat input to the gas, one on a negatively sloped branch and the other on a positively sloped branch. The data recorded during initial testing indicated operating points on both branches of the steady-state curve.

ACKNOWLEDGMENTS

TABLE OF CONTENTS

Chapters

LIST OF FIGURES

CHAPTER I

INTRODUCTION

A. Definition of Problem

The design and development of a successful solid core reactor

for nuclear propulsion, like every new engineering endeavor, has been

accompanied by numerous problems. Its requirements of light weight,

compact size, and high power density for use in rockets and aircraft

have led to many difficulties not encountered during development of

power reactors for land and ship installation. This report deals

primarily with one of these problems, namely the "laminar instability"

phenomenon which so far has been theoretically predicted but has not,

as far as is generally known, been observed during actual testing.

Calculations have shown it to be associated with the low-flow

conditions which may occur during cool-down of the solid-core, gas-

cooled reactor. The gas often used as the coolant/propellant in

nuclear rockets is hydrogen due to the light weight, high specific

impulse requirements.

A cutaway sketch of a solid core nuclear rocket is shown in

Figure 1. The following table gives typical full power data

gathered by the Los Alamos Scientific Laboratory during a test of the

hydrogen-cooled Kiwi B-4E reactor[1]:

Reactor Thermal Power	891	Mw
Reactor Flow Rate	69.3	lbm/sec
Nozzle – Inlet Pressure	779	psia
Core-Inlet Pressure	580	psia
Core-Outlet Pressure	497	psia
Reflector-Inlet Temperature	∿110	°R
Core-Inlet LH$_2$ Temperature	170	°R
Fuel Element Average Exit Temperature	4040	°R

Under these full-power conditions, flow rates and pressures are high, flows are turbulent, laminar flow problems are avoided. The potential problem is encountered when the reactor after running for a time is shut down. With the coolant turbo-pump no longer functioning, pressures are reduced to the order of one atmosphere; flows are reduced; temperatures of the coolant entering the reflector become low due to decreased cooling requirements in the nozzle. Heating in the reflector however is still present because of Gamma decay radiation from the fission products. This heat source may be significant for a period of a few minutes to several hours, depending upon the length of time the reactor was run at full power.[2]

It is these shut-down conditions that give rise to a possible laminar instability. Figure 2 shows a typical steady state operating curve[3] for hydrogen flow in a single thin tube under the above shut-down conditions. Seen from this curve is the fact that for a given

pressure drop and heat rate to the gas, two possible flow rates exist. The larger corresponds to all turbulent flow within the tube; the smaller corresponds to a laminar exit flow condition. Subsequent stability analysis which will be outlined in the next section indicates that an operating point on the low-flow, negative-slope branch of the curve exists in a state of unstable equilibrium. For a given pressure drop a perturbation involving a slight decrease in flow rate produces a flow excursion toward still lower flow rate. The resultant high tube temperatures would lead to possible failure of the tube. A perturbation to slightly higher flow rate gives rise to an excursion to a stable operating point on the positively-sloped branch of the steady-state characteristic.

An actual laboratory occurrence of this dynamical flow phenomenon remains to be observed. Therefore it has been the purpose of this project to design and construct apparatus with which the existence and nature of this flow phenomenon could possibly be investigated. If observed, then the apparatus could also be used to study various means of achieving stable operation at the low-flow condition.

B. Previous Work

An extensive set of steady-state operating conditions were computed by Harry[3] by numerical integration of the one dimensional conservation equations (mass, momentum, and energy) using a stepwise

iteration technique. At each step, the state equation for para-hydrogen was solved independently from known empirical data. Harry's method is described in more detail in Appendix B.

A typical set of results for uniform heat input over the length of the tube is given in Figure 3. The dotted portions of the curves indicate where dissociation although neglected, may be significant. The transition zone shown in the figure indicates the range of inlet Mach numbers $(M_1 \ \alpha \ W/A)$ over which transition from turbulent to laminar flow within the tube occurs. This transition is associated with the reduction in Reynolds number below about 1000 due to the increase in temperature and viscosity of the gas while flowing through the tube.

To obtain further insight into the nature of the steady-state solutions Harry[3], using various simplifying assumptions, again integrated the flow equations (B1, B2, B3) over the length of the tube. This closed form approximation, also described in Appendix B, is similar to that discussed in reference 2 and others. The resulting criterion (i.e., a necessary condition) for the occurrence of a negative slope (from equation B6) is that $(3-n)\tau - (mn+2)(\tau-1) \leq 0$ if τ is assumed large. The conclusion drawn is that for hydrogen gas, a negative slope and therefore unstable flow may occur for $\tau > 5$.

As an aid in design, Harry presented some numerical results in terms of dimensionless groups obtained from the approximate steady-state equations. These groups are defined in Appendix B.

One important conclusion can be drawn from Harry's steady-state analyses. It was shown that the minimum pressure drop occurs at flows and pressure drops just less than those at which flow in the tube is entirely turbulent. Therefore the "rule of thumb" is suggested that "the laminar instability is potentially a problem whenever any part of the heated section has laminar flow."[3]

Some degree of experimental verification of the steady-state characteristics was obtained by Turney and Smith[4] who ran experiments using normal hydrogen flowing in an electrically heated Nichrome tube having dimensions of 50" x .116" ID. Using inlet conditions of $P_1 = 10$ psia and $T_1 = 140°R$, operating points on both branches of the steady state curve were found.

Tests conducted by Guevara, McInteer and Potter[5] at the Los Alamos Scientific Laboratory again showed that operating points on both branches could be observed. These tests used helium gas flowing in electrically heated capillary tubes whose inside diameters were on the order of .012".

An analysis of the flow dynamics has been presented only recently by Reshotko[6]. This work verifies the correctness of the

criterion for instability and provides equations from which growth
rates and excursion paths can be calculated for any reactor whose
steady-state characteristics are known.

Reshotko's theory involves two basic assumptions. First, that
the characteristic flow time is very long compared to the time for
an acoustic disturbance to travel the length of the tube
(or, $M \ll 1$) . Consequently, the transient flow could be treated
as a succession of steady state conditions. The second assumption
is that thermal response time of the tube wall structure is
comparable to characteristic flow time. Thus, the time dependent
term was retained in the equation governing the energy balance of
the core. Under these assumptions the pertinent equations reduce
to a single first order differential equation describing the
variation of $\overline{Q}$, the average heating rate to the gas, as a function
of time.

Reshotko's analysis found that operating points on the
negatively sloped portion of the curve were points of unstable
equilibrium. An excursion at constant Δp away from the curve
would continue in the direction of the initial perturbation. He
found that points on the right branch where slope is positive and
flow is turbulent are in stable equilibrium. It was concluded
further that the flow instability encountered is not a hydrodynamic
instability at all. Instead it is associated with the thermal

response of the core and the heat transfer characteristics of the flow. For a typical reactor geometry having the steady state characteristics of Figure 3, excursion times were found to be of the order of minutes to hours and varied as the heat capacity of the reactor core.

Looking at Figure 3, some physical explanation can be given in support of the unstable nature of the negatively sloped portion of the steady-state characteristic. A point on this branch when perturbed to a higher flow rate (at constant pressure drop) requires more heat to the gas since it is now on a higher Q curve. This additional heat is supplied from the associated cooling of the core, and the excursion continues. Maximum heating rate corresponds to that operating curve which is tangent to the excursion path. A decrease in flow from the lower branch also causes an excursion. Since lower flow would demand a lower heat rate to the gas, the balance of the reactor heat release would go to heating the core. On the right branch, increased flow would require less heating rate to the gas, but cooling of the core increases heating rate. Consequently, the flow must return to its original operating point.

C. Further Consideration

While the previous section has covered the most important aspects of the "laminar instability" problem, there remains one area in which further investigation may be of interest. This is

consideration of the behavior of the steady state pressure vs. flow
rate curves near the origin.

It seems plausible to assume that zero flow rate should be
accompanied by zero pressure drop, a behavior observed for zero
heating. Following this line of reasoning one would expect the
curve in Figure 2 to return to the origin for low flow rates as
shown in the sketch:
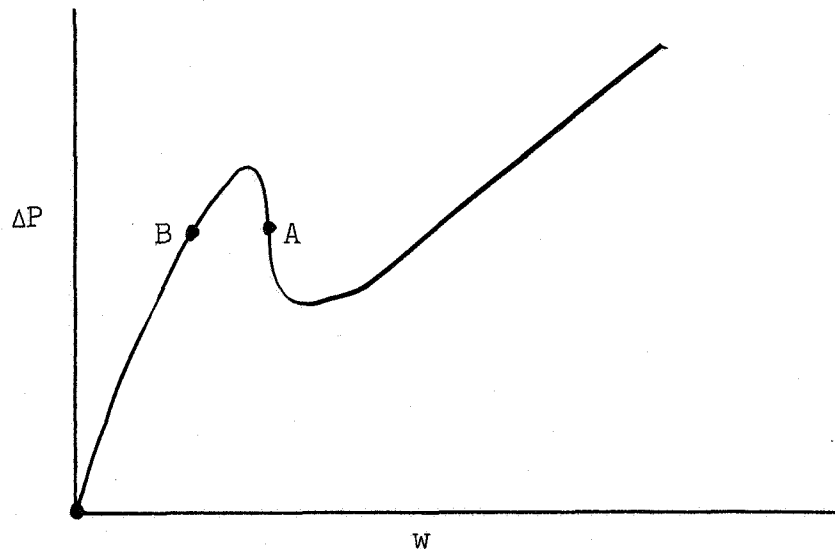
Following the criterion of stable behavior for positive slope,
a flow excursion toward lower flow from point A would be expected
to settle on a new stable equilibrium point at B .

The Los Alamos study[5] presents experimental results which when
plotted describe just such a curve; it states further that
"theoretical considerations would anticipate curves with a shape

such as .... (that in the sketch above)". These "theoretical
considerations" however have never been published and nothing more
is said about any method of derivation.

It is impossible to predict the existence of this low flow
branch from Harry's analysis. His starting equations make use of
a friction factor f which along with viscosity increases
monotonically with temperature. Rewriting equation B5 as:

$$p\Delta p = Xw + Yw^{3-n}\{1 + Zw^{-1}\}^{mn+2}$$

where C_p, n, m, X, Y, Z are assumed constant, it is seen that
for $w \rightarrow 0$, the friction pressure drop term blows up as long as
$mn + n - 1 > 0$. From this argument it is seen that for positive
viscosity-temperature exponent m , a negative slope prevails as
long as n takes on a laminar value and C_p is more or less
constant. Such behavior prevails until dissociation begins; in
hydrogen this is up to temperatures on the order of 3500°R. With
dissociation and subsequent ionization come new trends in the
viscosity-temperature relations. The viscosity exponent m drops
to a very low positive value through the range of dissociation[2]
(for hydrogen at 1 atm pressure), but then increases once
dissociation is complete. A similar behavior is said to be
followed upon ionization, but further study at these temperatures
becomes merely an academic exercise; the physical limitation of the

structure is approached, and some previous assumptions like no radial heat transfer break down.

The search for operating points on this low flow branch will be considered an objective of the experimental program.

CHAPTER II

EXPERIMENTAL PROGRAM

A. Proposed Work

The major objectives of the present work were the design,
construction, and testing of an apparatus which could enable study
of both the static and dynamic phenomena occurring in parallel
reactor passages. A tube bank consisting of one, two, and possibly
three heated flow passages was planned. It was felt that these
passages when connected to common headers would closely simulate a
reactor reflector.

Using at first only one tube in the apparatus, Reshotko's
predicted flow excursion phenomena could be investigated. Possibly
it would be desired to run the apparatus with different tube lengths
and diameters in order that the effect of these variations could be
recorded. The operation of the experiment with two parallel tubes
would allow the experimenter to determine if in adjacent tubes
under the same conditions two different flow rates could be made to
exist simultaneously; if so, the manipulations necessary to produce
this phenomenon could be learned.

Before actual apparatus design could begin, various preliminary
calculations of flow characteristics accompanying different gases,

tube geometries, and heating rates were performed. Use was made
of the non-dimensional parameters formulated by Harry (Figure 4)
to get rough results. Although hydrogen gas is the fluid of
primary consideration in the actual nuclear rocket case, it was
rejected as the working medium for the reason that it is explosive
if heated and mixed with air. Helium gas was found through
preliminary calculations to exhibit much the same flow behavior
under safer, more easily maintained and measured conditions.
Helium is a desirable gas to use because it is inert and because
many of its properties like conductivity, heat capacity at constant
pressure, and viscosity are relatively close to those of hydrogen
(Ref. 7, 8, 9, 10).

An inlet temperature of 140°R was selected as the lowest
temperature which could be easily obtained; it is the temperature
of boiling liquid nitrogen.

With the preliminary estimates made, a calculation of pressure
as a function of flow rate was performed using equation B5 from
Harry's analysis. Dimensions of available tubing, assumed
conditions of inlet pressure and heating rate, and friction factors
of $16/Re$ for laminar flow and $.117/Re^3$ for turbulent flow[*] were

---

[*]This value of turbulent friction factor follows quite closely
the curve defined by the modified Karman-Nikuradse relation,
equation B4.

used. The results are shown in Figure 5, the dashed line being an assumed curve in the transition area.

Theoretical prediction of flow excursions resulting from perturbation from the steady state curves were possible using some results of Reshotko's analysis. In particular the time history of a flow excursion for a uniformly heated passage may be calculated using the following equation[6]:

$$\mathbb{T} = \int_{\tau_i}^{\tau} \frac{\frac{d\overline{Q}}{d\tau}\left\{1 + XY - (1-n) \frac{d\ell n(\frac{W}{A})}{d\ell n \ \overline{Q}}\bigg|_{\Delta P}\right\}}{\frac{h_1}{(h_1)_o}\left[\frac{\tau^{mn+1} - 1}{(\tau-1)(mn+1)}\right][\overline{Q}_o - \overline{Q}]} d\tau \tag{1}$$

where

$$X \equiv \left[\frac{h_1 T_1}{\overline{Q}}\left(\frac{(mn+2)(\tau-1)\tau^{mn+1} - (\tau^{mn+2}-1)}{(mn+1)(mn+2)(\tau-1)}\right) - mn\left(1 - \frac{\ell n \ \tau}{\tau-1}\right)\right]$$

$$Y \equiv \left[1 - \frac{d\ell n(\frac{W}{A})}{d\ell n \ \overline{Q}}\bigg|_{\Delta P}\right]$$

$\mathbb{T}$ is a dimensionless time defined $\mathbb{T} \equiv \frac{1}{\partial m} \ \frac{A}{ar_h}\left(\frac{h_1}{c}\right)_o t$

and the subscript "o" denotes condition at the unperturbed steady operating point.

Using graphical methods beginning with the steady-state curves of Figure 5 and accompanying temperature ratios, the integrand of equation (1) can be plotted as a function of τ . This curve is then integrated graphically to obtain the results plotted in Figures 6 and 7. An excursion to both higher and lower flow rates at a constant pressure drop of $\Delta P = 2$ psi is shown. The starting point in both cases was on the lower branch of the $\overline{Q} = .7 \frac{Btu}{sec\ ft^2}$ curve, and an initial perturbation from $\overline{Q}_o$ of about 3.2% was used. As seen in Figure 6, the time involved in going from the unstable to the stable branch is on the order of 150 dimensionless time units. Using the properties of the proposed construction materials, one time unit T is 5 seconds; $150\ T = 12.5$ min.

From the previous discussion it is seen that an experiment performed with helium could not only demonstrate sufficiently all the aspects of the flow phenomena, but it could do so with a lesser degree of experimental difficulty. This is due to the higher pressure drops and flow rates, and lower temperature ratios predicted for helium in the area of interest.

B. Apparatus Design

The initial design and construction was done with a view toward experimentation with only one test section. However flow rate predictions and plenum design were done in such a way that two parallel tubes could be used in future operation.

It was decided early in the project that a closed loop system would be used (see Figures 8 and 9). The reason for this was simply that a closed system would be more economical.

The test section was made from available Nichrome V (80% nickel, 20% chromium) tubing. Its dimensions of .094 inch inside diameter, 4 1/2 foot length, and .020 inch wall supported desirable flow characteristics (Figure 5). The big advantage of Nichrome was its small variation of resistivity with temperature, making electrical resistance heating a good method of obtaining a "heated reactor passage."[*]

In an effort to minimize heat losses which in general would increase with an increase in wall temperature, the test section was placed in a vacuum tank whose pressure was sufficiently low to eliminate significant convection heat transfer from the outside of the tube. Thermal expansion of the tube required use of a spring suspension system which would maintain a tension on the tube at all times. This and the presence of a liquid nitrogen heat exchanger necessitated the placing of the entire assembly, i.e. heat exchanger,

---

[*] Data[11] indicates that the resistivity of heavy Nichrome wire will increase no more than a few percent during heating from room temperature to 2000°F. While this variation would lead to some non-uniformity in heating rate, it would not effect the nature of the experiment.

test section, inlet and outlet plenums, inside the vacuum tank. The tank and assembly are shown in Figures 10 and 11.

As seen in Figure 8, pressures in the inlet and outlet plenums were to be controlled by regulators whose inlet flow would be supplied from a high pressure reservoir. Another low pressure or vacuum reservoir in the line upstream of the circulating pump would provide a low pressure dump for the flow leaving the test section and outlet plenum regulator.

Gas temperatures in the inlet and outlet plenums were measured by copper-constantan and shielded chromel-alumel thermocouples respectively. Five thermocouples silver-soldered to the test section enabled wall temperature profiles to be measured. Pressure drop across the test section was read from a transducer indicator; all other pressures of interest were measured with gauges. Instrumentation is pictured in Figures 9 and 12.

The primary limitation of the design is the silver solder on the test section. At a wall temperature of approximately 1260°F, the thermocouples would begin melting off. Since this would correspond to a temperature ratio τ of about 12, somewhat above that at which meaningful data could be taken, it is not considered an immediate problem. With the equipment in use

during initial testing, it would be possible to operate with an
inlet pressure p , between O and 5 psig, a pressure drop ΔP
of up to 10 psi, and an electrical power capacity corresponding to
a heating rate Q of up to .85 Btu/sec ft^2 (assuming uniform
heating with no losses).

C. Experimental Procedure

The initial step to be taken before excursion data can be
recorded involves the procedure necessary to get the tube operating
on the unstable branch. The mere observation of the ease or
difficulty encountered will be worthwhile.

Since this negatively-sloped branch was predicted by Reshotko
to be unstable for constant pressure but not for constant mass flow
rate, the following procedure will be used:

A flow regulator made up of a pressure regulator-throttling
valve combination shown in Figure 8 is adjusted to maintain a
constant flow rate at zero heating rate. This operating condition
is represented by point A in Figure 13. The heating power is then
turned on and the downstream regulator is simultaneously adjusted
to maintain a constant P_1 (and consequently a constant flow rate).
The steady-state operating condition then moves to point B. Using
the same heat input, this procedure is repeated for many different
flow rates to describe a steady state curve.

Once an operating point on the negatively sloped branch is realized, the upstream throttling valve is opened while simultaneously closing the pressure regulator (P_1 remaining unchanged) so that excursions at constant pressure drop can be observed. An excursion to lower flow rate will be followed as far as is prudent with respect to material limitations or as far as the operating point will go. An excursion to higher flow rate will be followed and recorded.

Once the shape of the steady-state curves is known, it would be interesting to investigate the behavior of an operating point situated below the ΔP_{min} point of a curve. Starting at point C of Figure 13, this could be done either by decreasing ΔP to point D or by increasing Q to Q_3. Since an operating point in this position would demand a smaller heating rate than that being supplied, it is guessed that an excursion to the left would result due to the excess heat going to raise the temperature of the tube.

CHAPTER III

RESULTS AND DISCUSSION

Results of initial testing are given in Figures 14 and 15.

Pressure drop and flow rates were recorded from the instrumentation.

Average heating rate to the gas was calculated from the equation

$\overline{Q} = (\frac{W}{A})C_p(T_{out} - T_{in})$. It is seen from runs 1 and 2 of Figure 14

that for a constant electrical power into the tube, the heating

rate to the gas, $\overline{Q}$, varied significantly over the range of flow

rates recorded. It is for this reason that the pressure drop curve

fails to directly indicate a negatively- sloped branch.

The results of these initial data runs prompted an investigation

of the amount of heat lost from the test section. These

calculations, outlined in Appendix C, made use of the wall temper-

ature profiles of Figure 15.

A preliminary estimate of the conduction along the tube

resulting from the gradients indicated in Figure 15 showed this

heat flow to be less than 1/4% of the average heat rate to the tube.

Calculations of Appendix C indicated that the convection loss

would at worst reduce the heating rate by only .01 Btu/sec ft^2 ,

about 1.3% of the heat rate to the tube. The radiation losses,

far more significant, are given in the following table:

19

Flow Rate ($\frac{W}{A}$) lbn/sec ft^2	Radiation Loss Btu/sec ft^2	(.85)-(Loss) Btu/sec ft^2
.907	.119	.731
1.307	.083	.767
1.854	.044	.806
2.490	.021	.829
3.182	.009	.841

The heating rates and losses, plotted in Figure 16, show there is still a significant loss which is unaccounted for. A run made with no electrical input to the tube (run 3 of Figure 14) showed there existed a heating rate to the gas of about 0.3 Btu/sec ft^2. This is now a "loss" into the test section and is of a magnitude comparable to the loss unaccounted for in Figure 16. This indicates that the mode of transfer is by conduction, possibly through the electrical and thermocouple wires which are attached to the tube.

In subsequent testing, several curves of Δp vs. W/A were plotted for different values of electrical heating rates. The average heating rate to the gas, $\overline{Q}$, was calculated for each point. From this set of results, the steady-state operating points having the same heating rate $\overline{Q}$ were connected, and a

double-branched set of curves similar to those in Figure 5 was
found. Excursions from points on the lower branch were not
detected.

The primary concern during future operation of the apparatus
will be the identification and elimination of the major heat
losses from the test section. This will perhaps enhance the
chances of observing flow excursions of the type described in
reference 6.

Summary

A discussion of "laminar instability" has been presented
with emphasis placed on the theoretical contributions of Harry[3]
and of Reshotko[6]. The results of these analyses were used to
design apparatus capable of studying the flow of gas in slender
heated tubes and possibly of providing a means for the observation
of flow excursions at constant pressure drop.

Results of early testing indicated very large heat losses
from the test section which led to a non-uniform heating of the
gas over the range of flow rates recorded. Nevertheless, it was
possible to find steady-state operating points on both branches

of the theoretically predicted curve.

Excursions from operating points on the lower branch were not observed in these experiments.
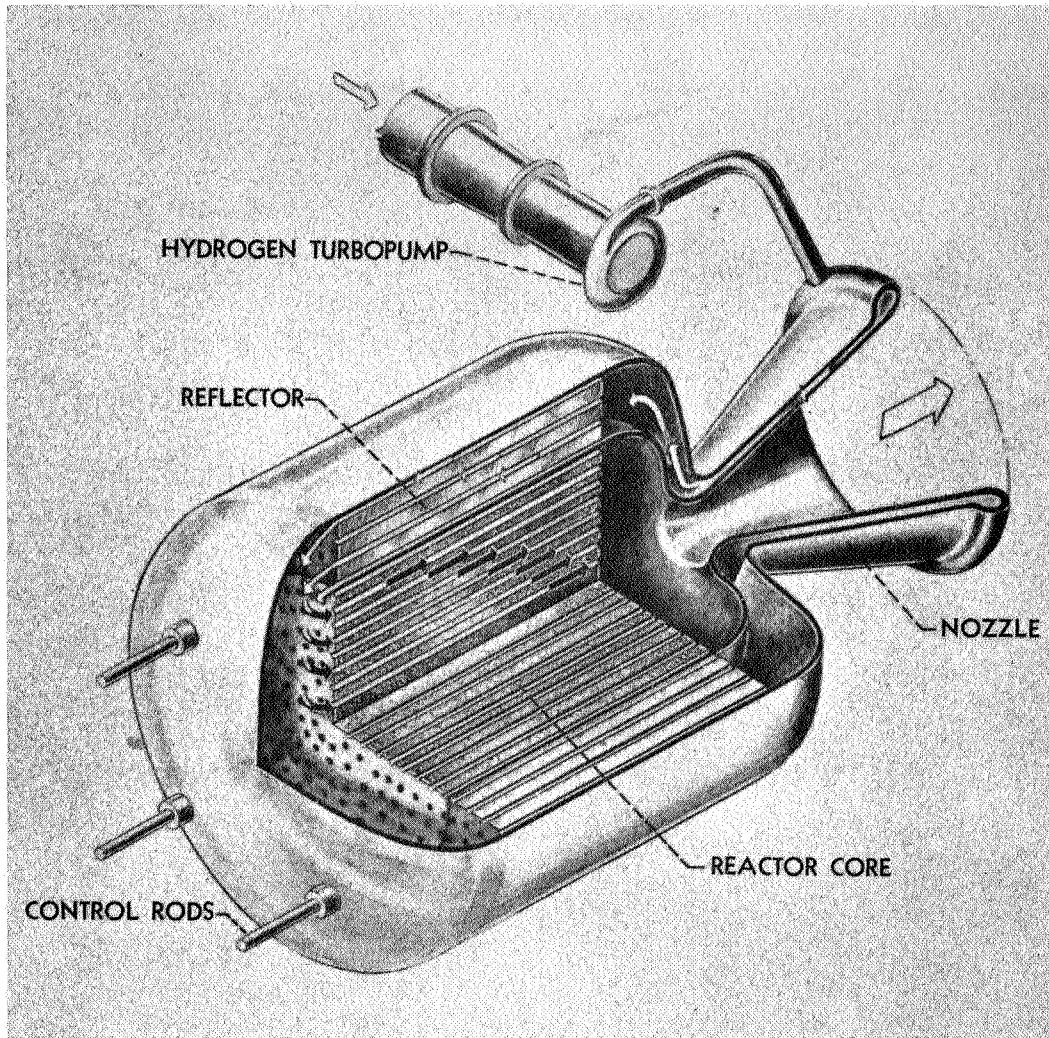
Figure 1. Cutaway Sketch of a Solid Core Nuclear
           Rocket Reactor
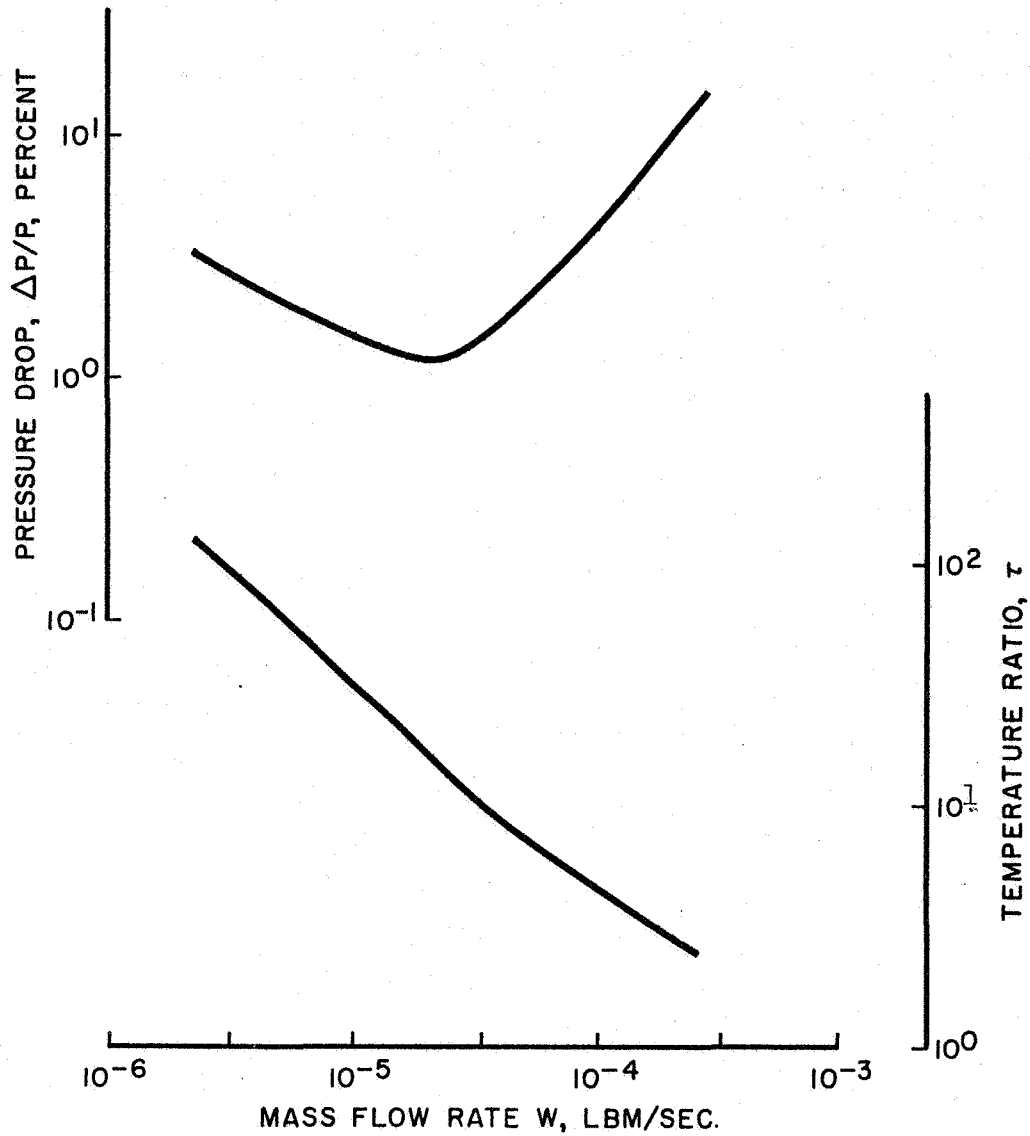   (From NASA Report SP-20)

Figure 2. Steady-State Flow Characteristics for Parahydrogen at
Typical Shut-Down Conditions
(From Harry[3])

Inlet Pressure, 20 Psia; Inlet Temperature, 50°R; Tube Diameter,
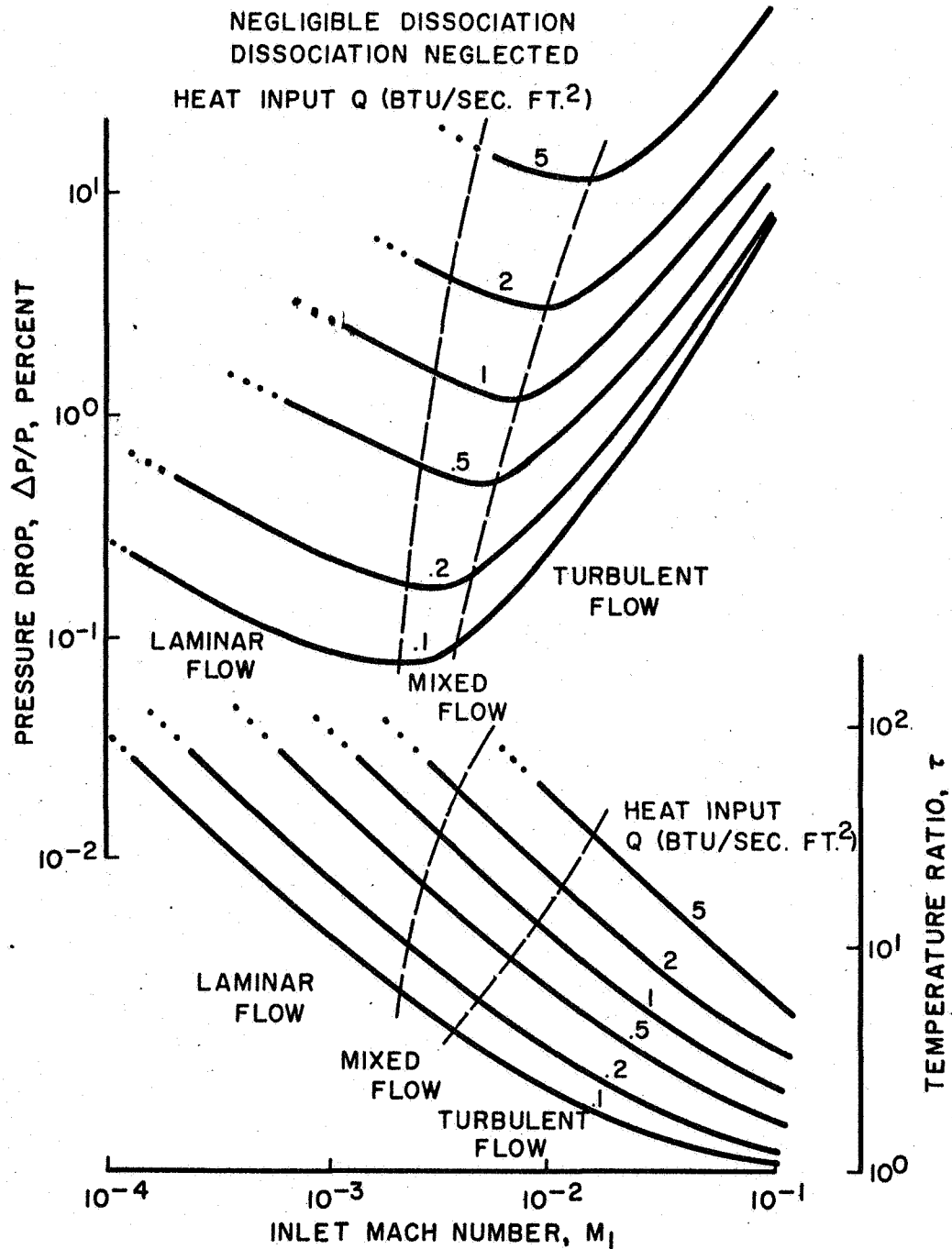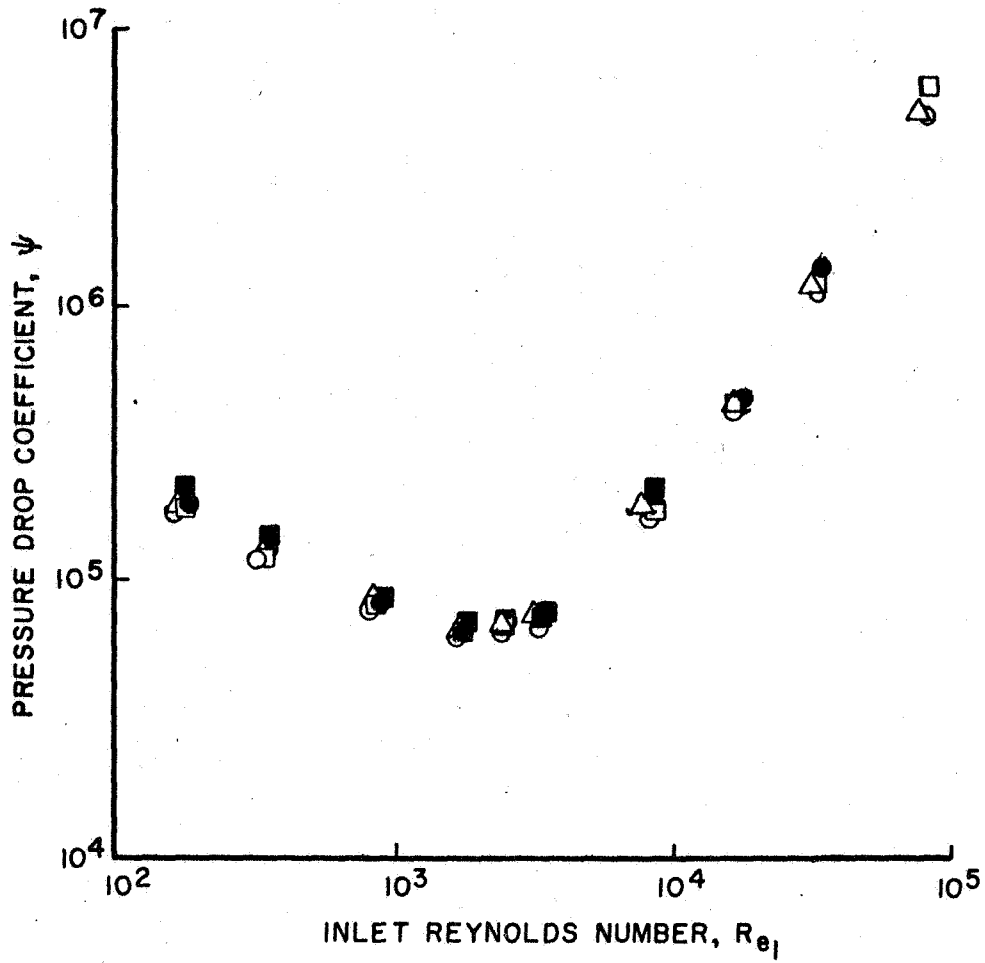0.10 Inch; Tube Length, 4 Ft.; Heat Input, 1 BTU/Sec Ft^2

25

Figure 3. Set of Steady-State Curves for Parahydrogen with Uniform Heating. Inlet Pressure, 20 Psia; Inlet Temperature, 50°R; Tube Diameter, 0.10 Inch; Tube Length, 4 Feet.

CASE	INLET PRESSURE PSIA	INLET TEMPERATURE °R	TUBE LENGTH FT.	TUBE DIA. IN.	HEAT INPUT $\dfrac{BTU}{SEC. \, FT.^2}$
○	20	50	4	.1	.1
□	10				
●	5				
■	2	↓	↓	↓	↓
△	20	2	2		.2

HEAT−INPUT COEFFICIENT, ϕ, 3400 ± 2 PERCENT

Figure 4.   Evaluation of Correlating Parameters
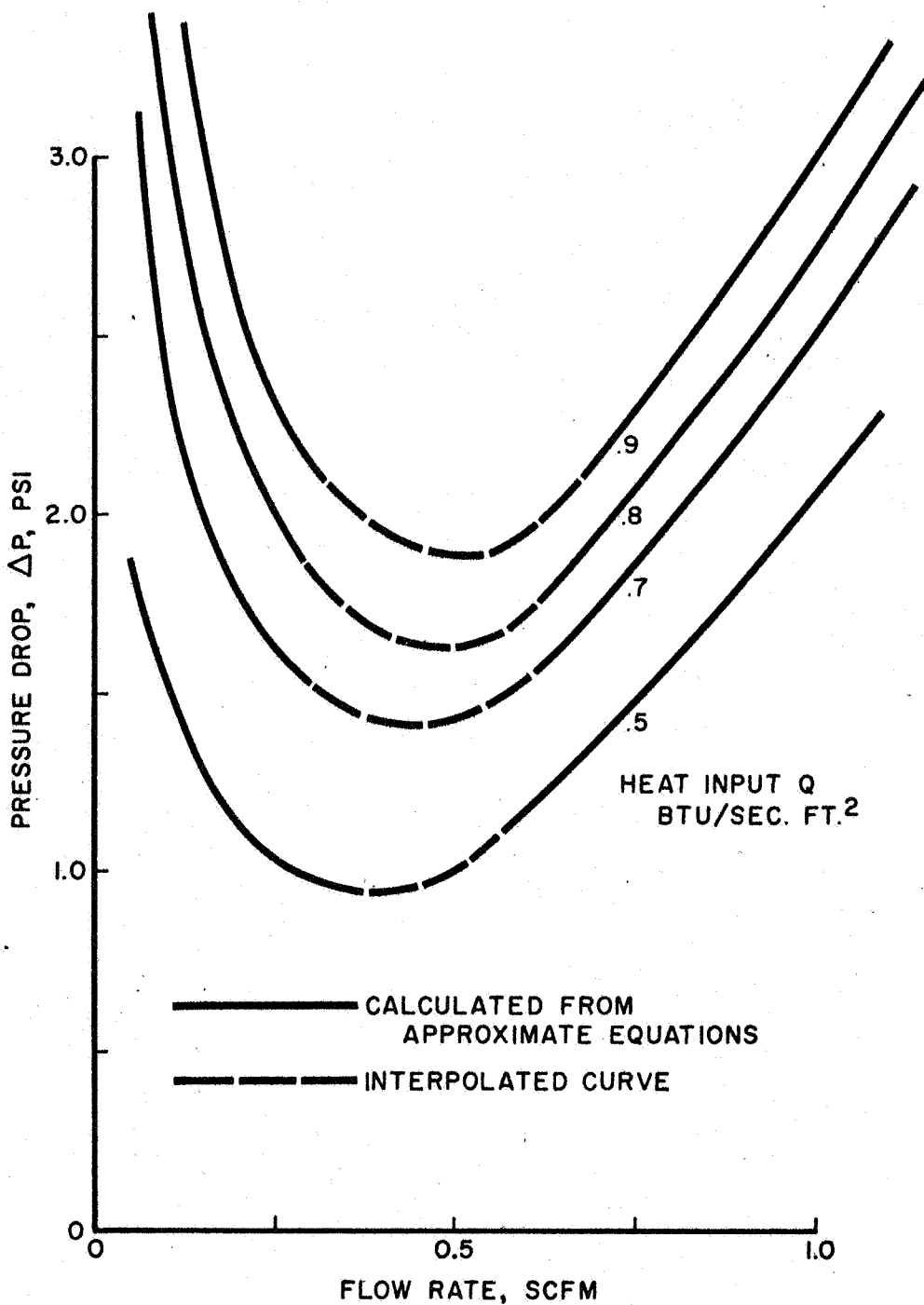
Figure 5.   Steady-State Flow Characteristics for Helium
            Inlet Pressure, 1 Psig; Inlet Temperature, 140°R;
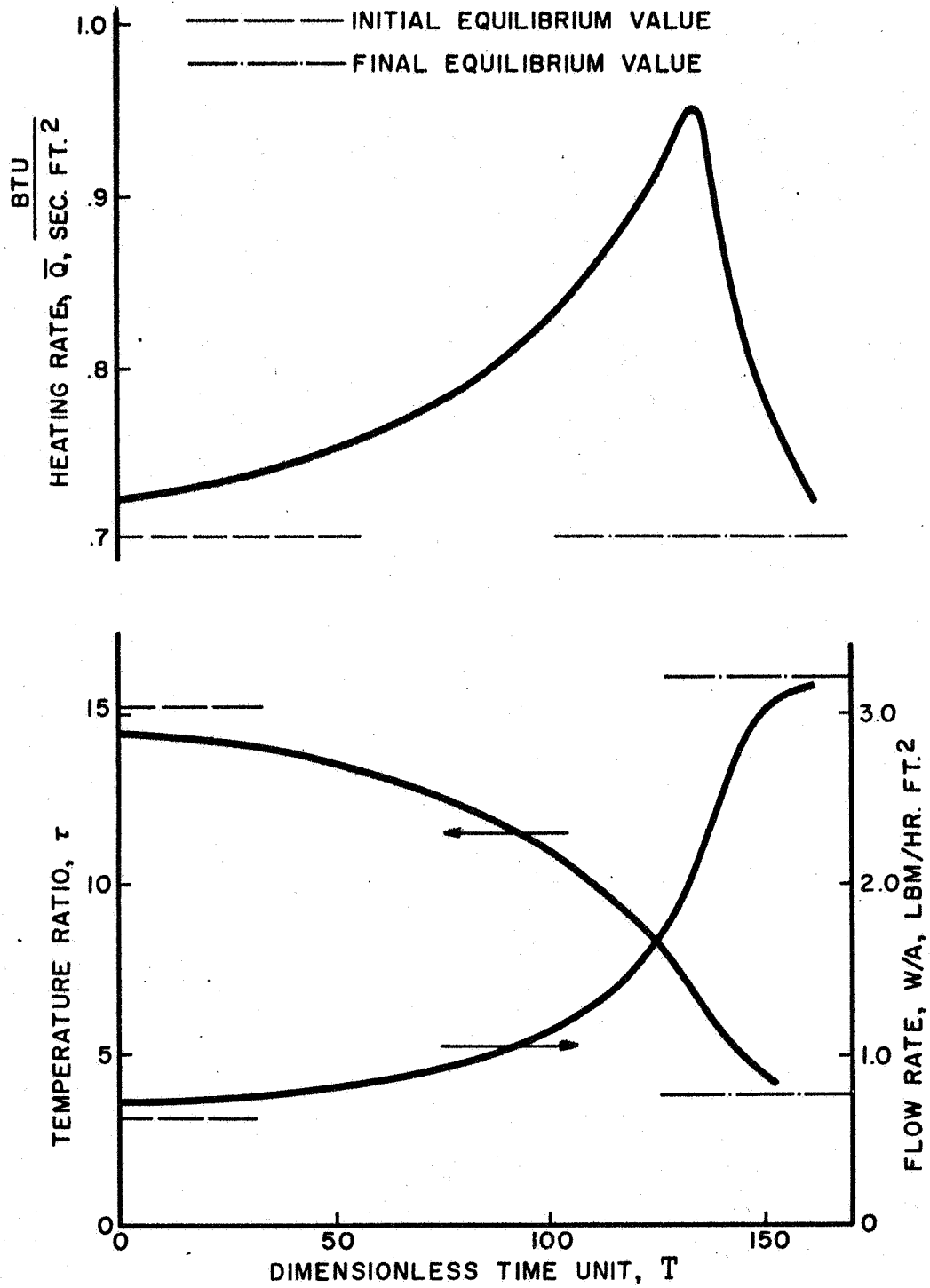   Tube Diameter, 0.094 In.; Tube Length, 4.5 Ft.
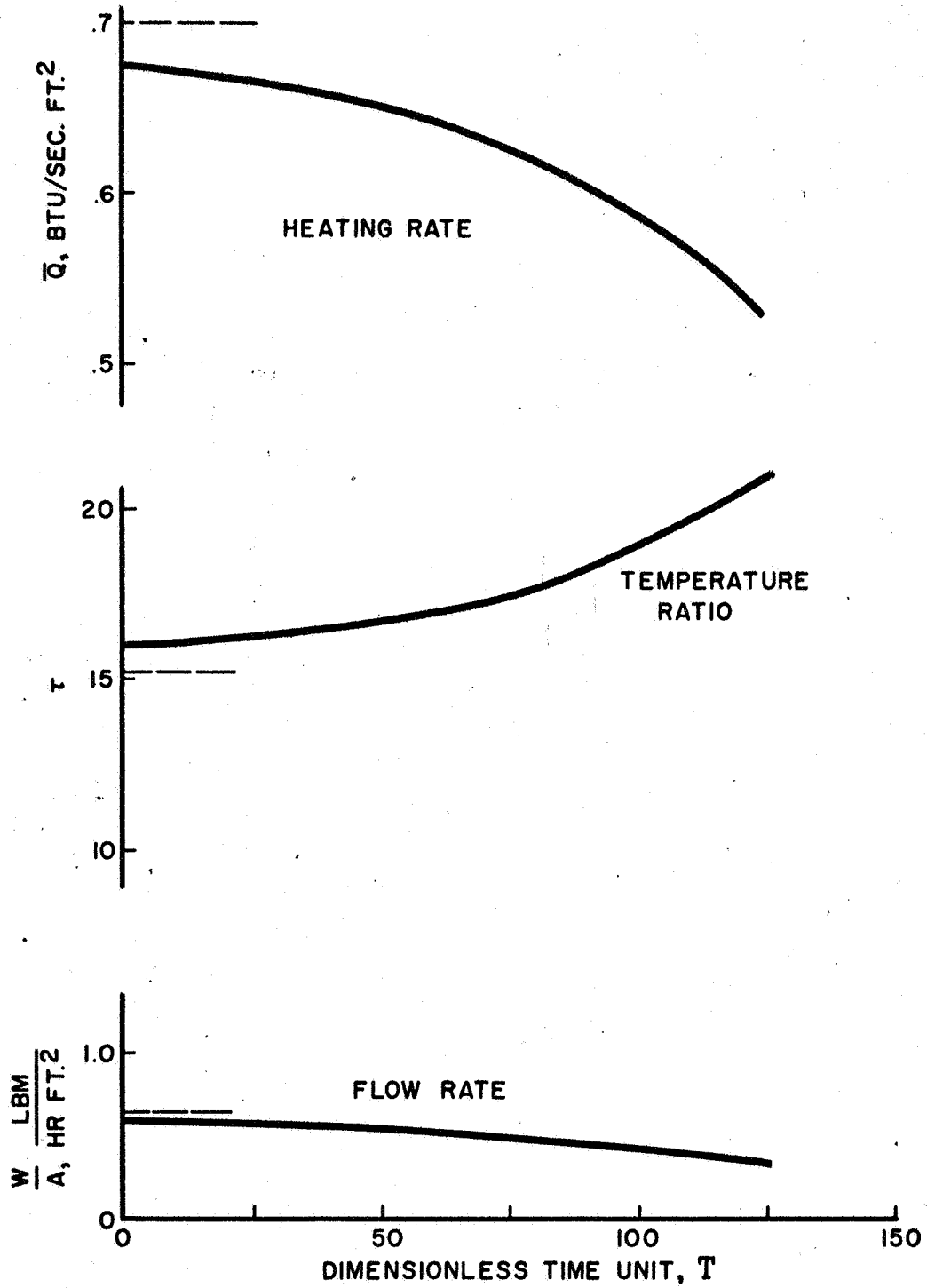
Figure 6. Excursion to Higher Flow Rate
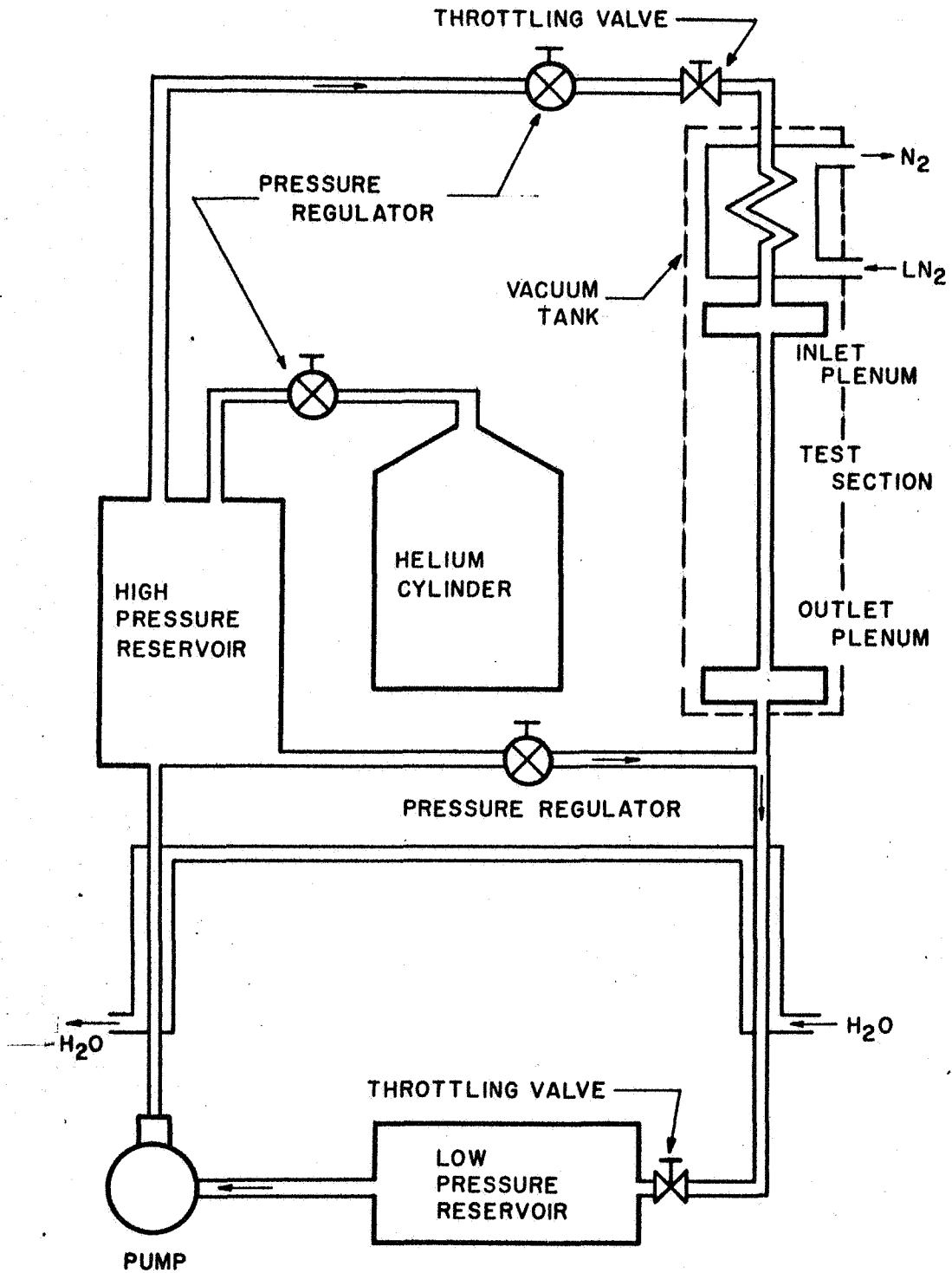
Figure 7. Excursion to Lower Flow Rate
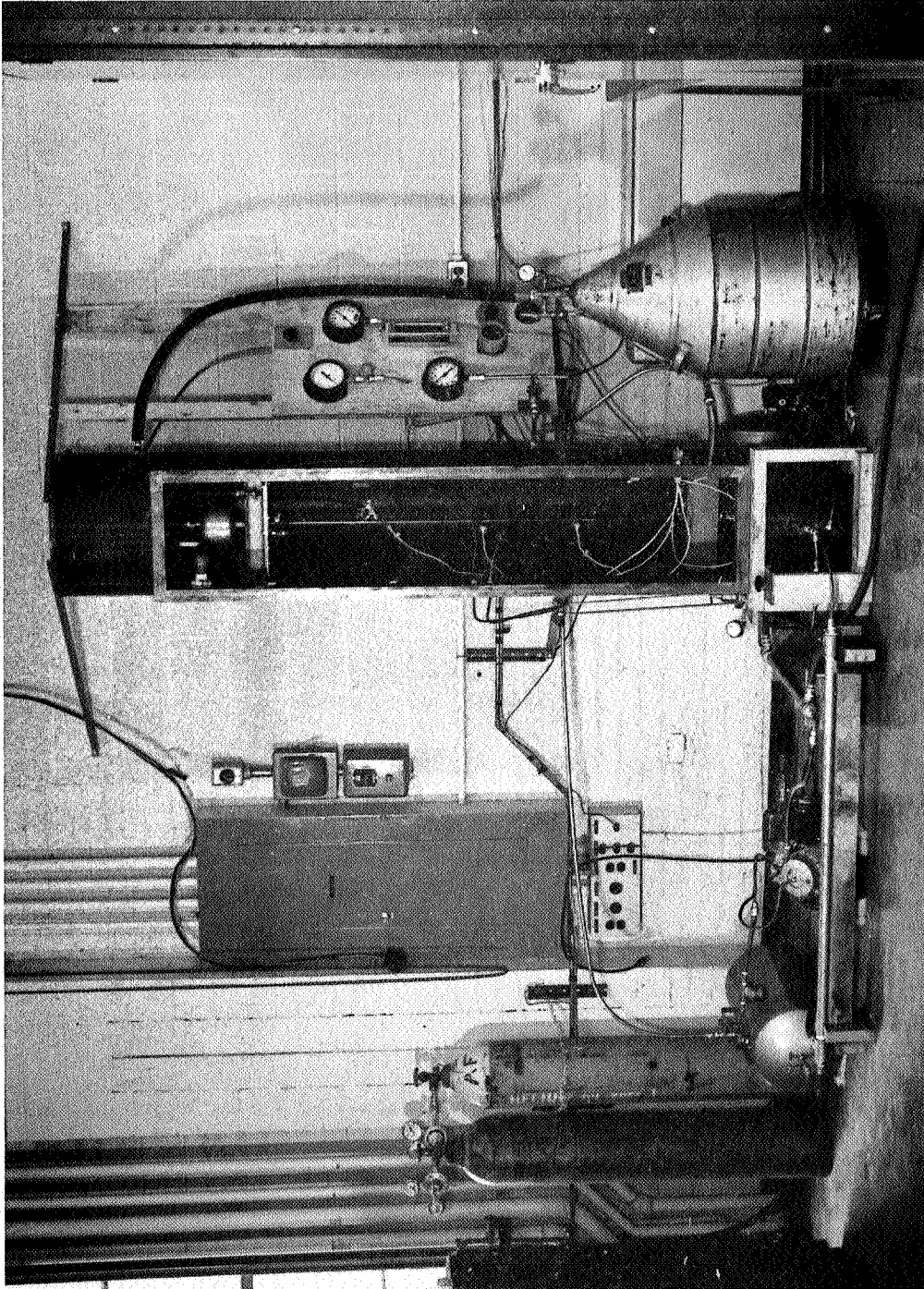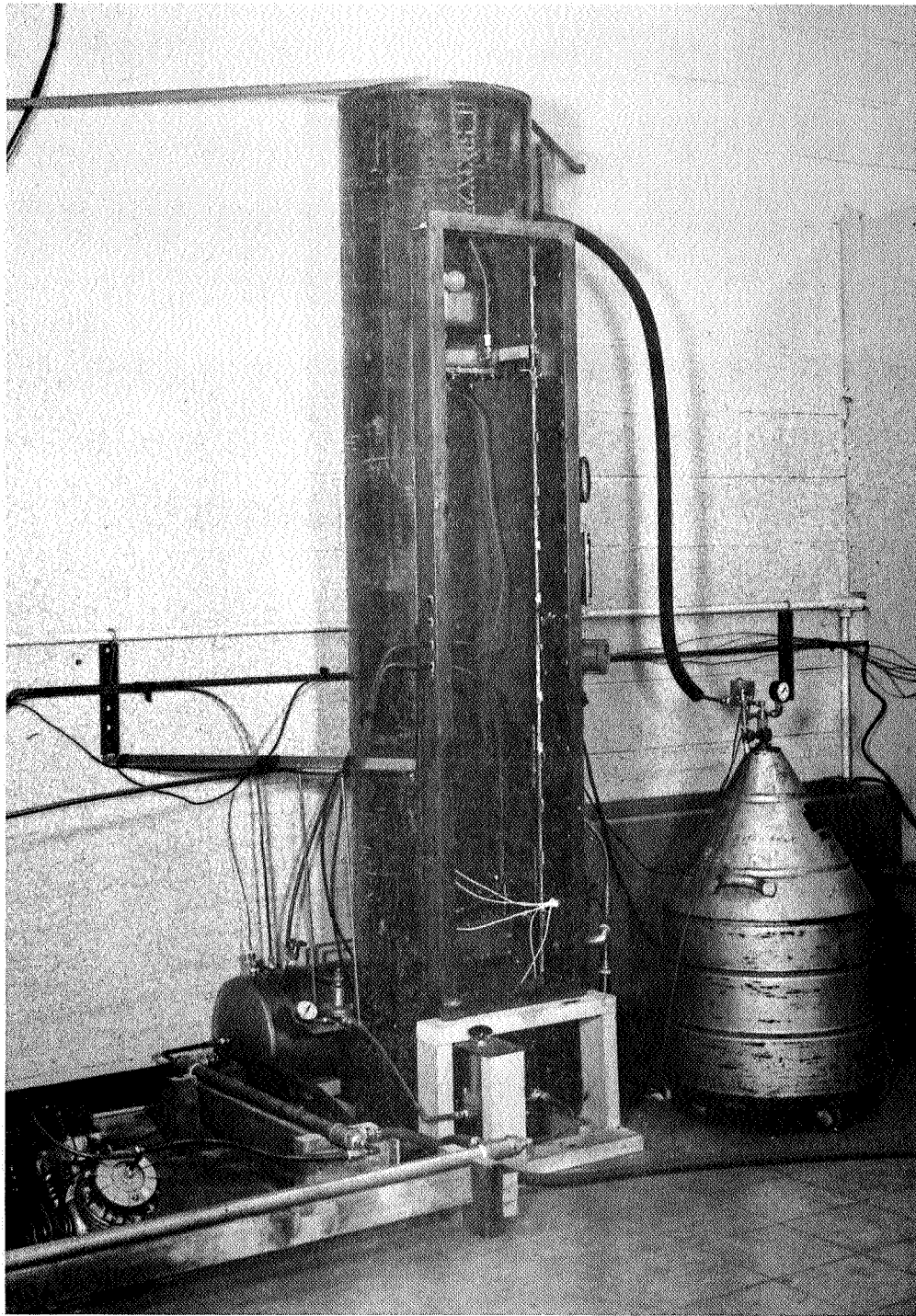
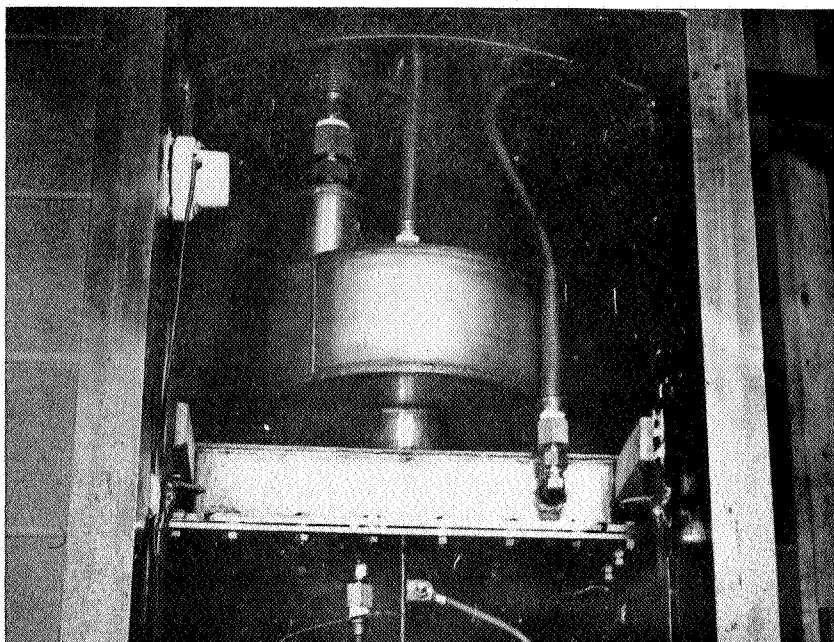Figure 8. Flow Diagram for Experimental Apparatus

Figure 9.

Figure 10. Vacuum Tank

Inlet Assembly
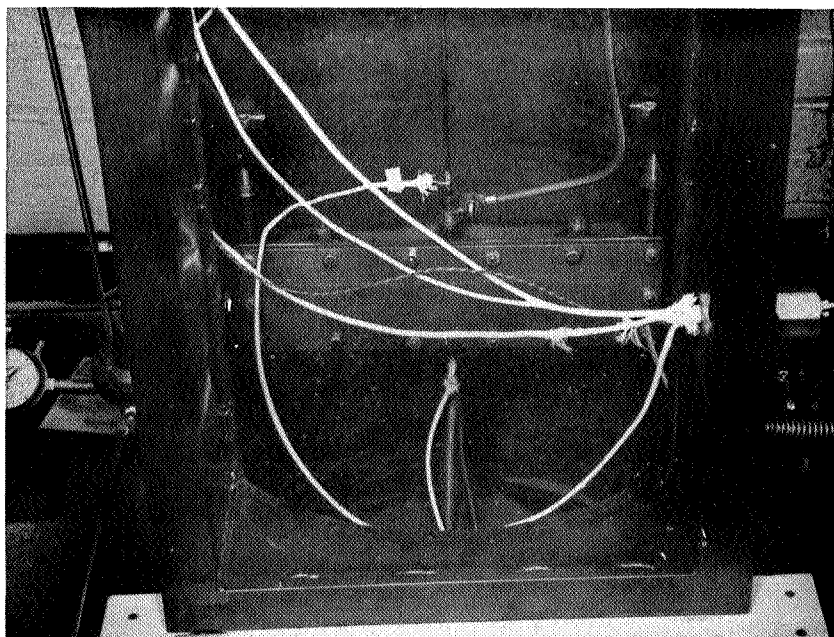
Outlet Plenum

Figure 11.
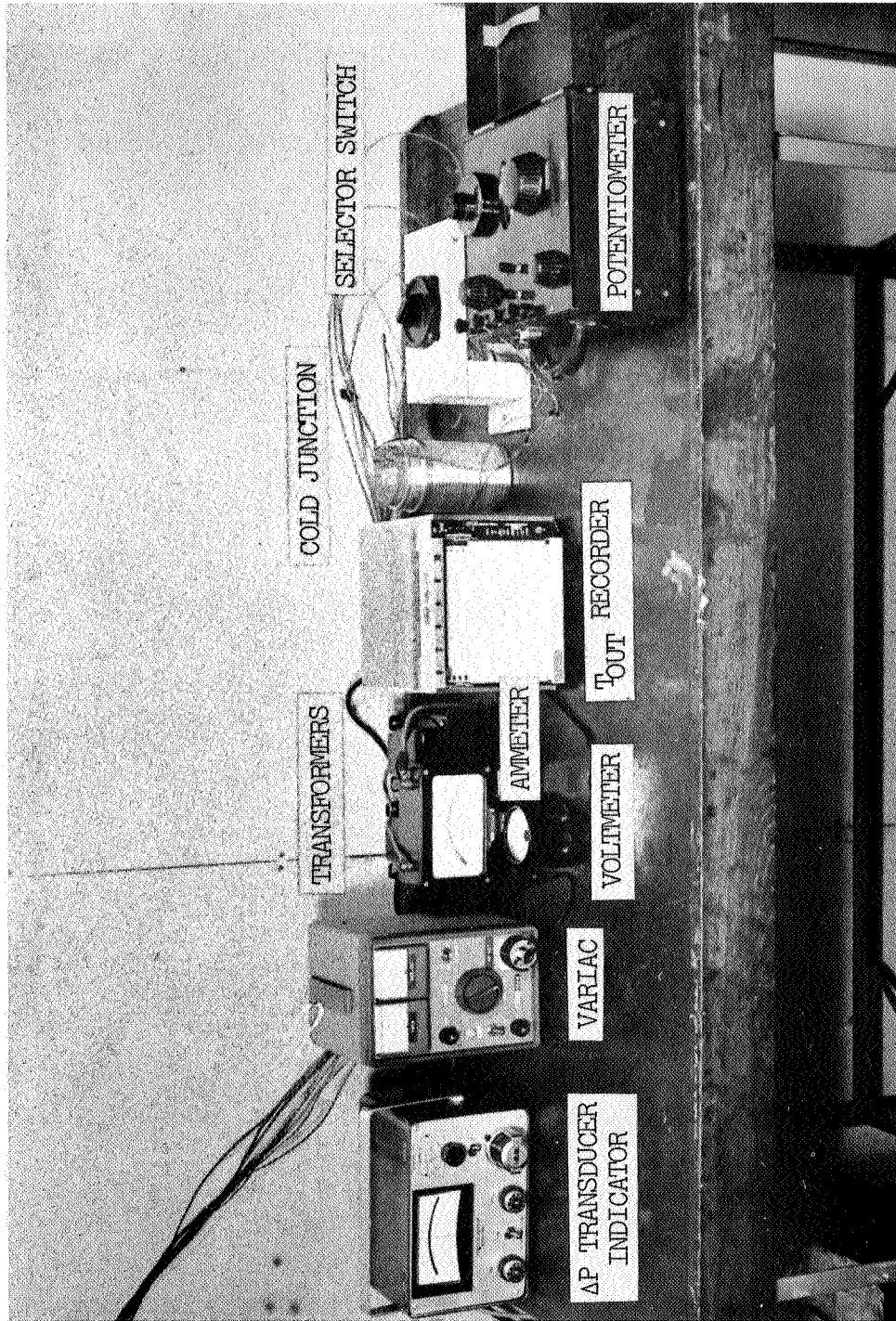
Figure 12. Instrumentation
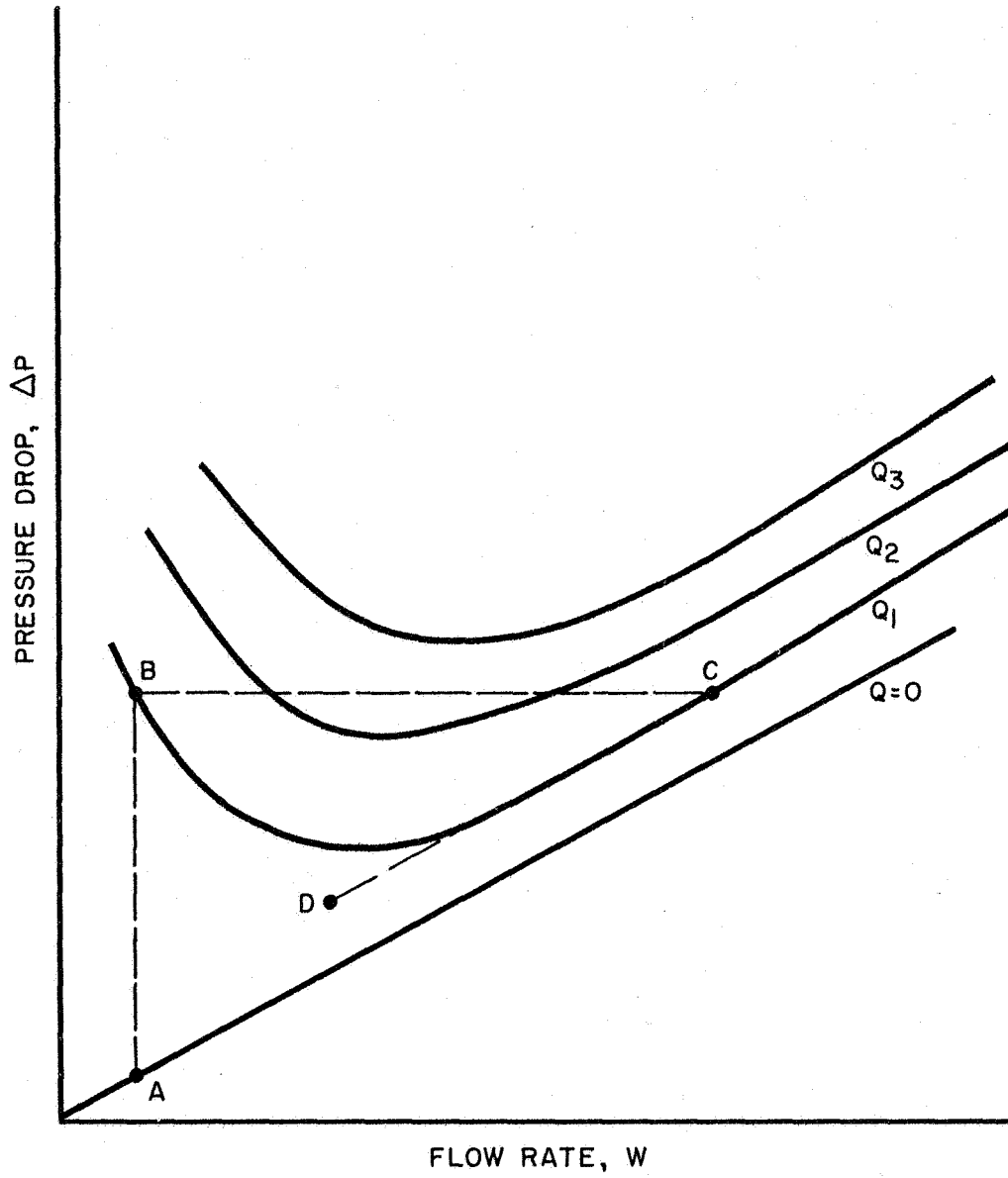
Figure 13. Description of Experimental Procedure

Run	Symbol	Electrical power input
1	△	0.866 Btu/sec ft^2
2	○	0.866 Btu/sec ft^2
3	□	0.0 Btu/sec ft^2
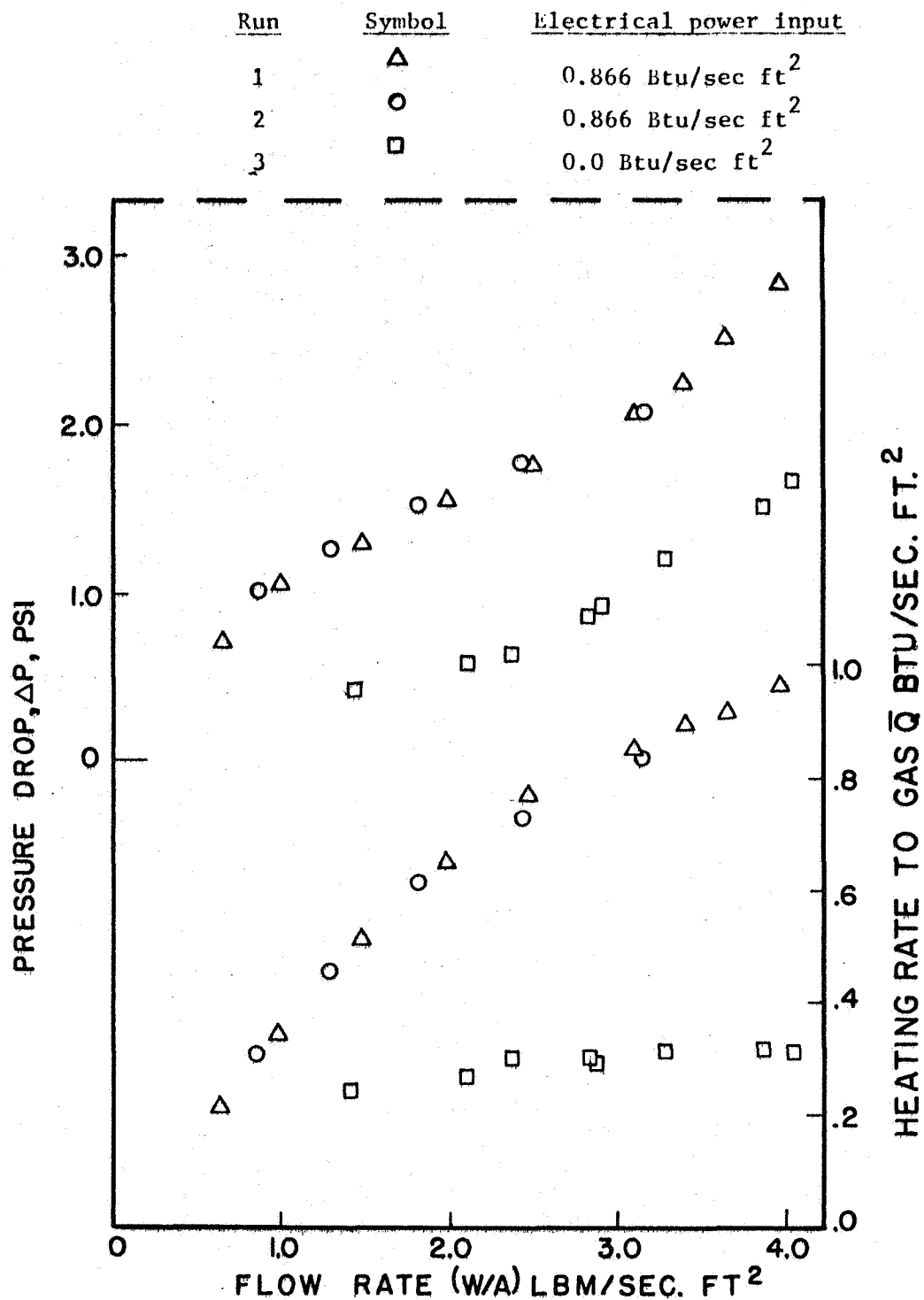
Figure 14. Experimental Results   Helium:
Inlet pressure , 1 psig; Inlet temperature, 140°F;
Tube ID, 0.094 inches; Tube length, 4.5 ft.

FLOW RATE, LBM/SEC. FT.^{2}

.897

1.295

1.837

2.46

3.15

32°F

RESULTING GAS
EXIT TEMPERATURE, T_2

$P_1 = 1$ PSIG

$T_1 = 140°R$

$D = 0.094$ INCHES

ELECTRIC POWER INPUT $= 0.86$ BTU/FT^{2}SEC.

TUBE WALL TEMPERATURE, T_w,°R

DISTANCE FROM TUBE ENTRANCE, X, IN

Figure 15. Wall Temperature Profiles for Run #2

Figure 16. Heat Distribution Along the Length of the Tube

APPENDIX A

SYMBOLS

A   Cross-sectional flow area

a   Cross-sectional area of "reactor core" associated with single passage

C   Sonic velocity

c   Specific heat of "core" material

C_p Specific heat at constant pressure

D   Tube ID

F   Geometric shape and emissivity factor for radiation from one gray body to another
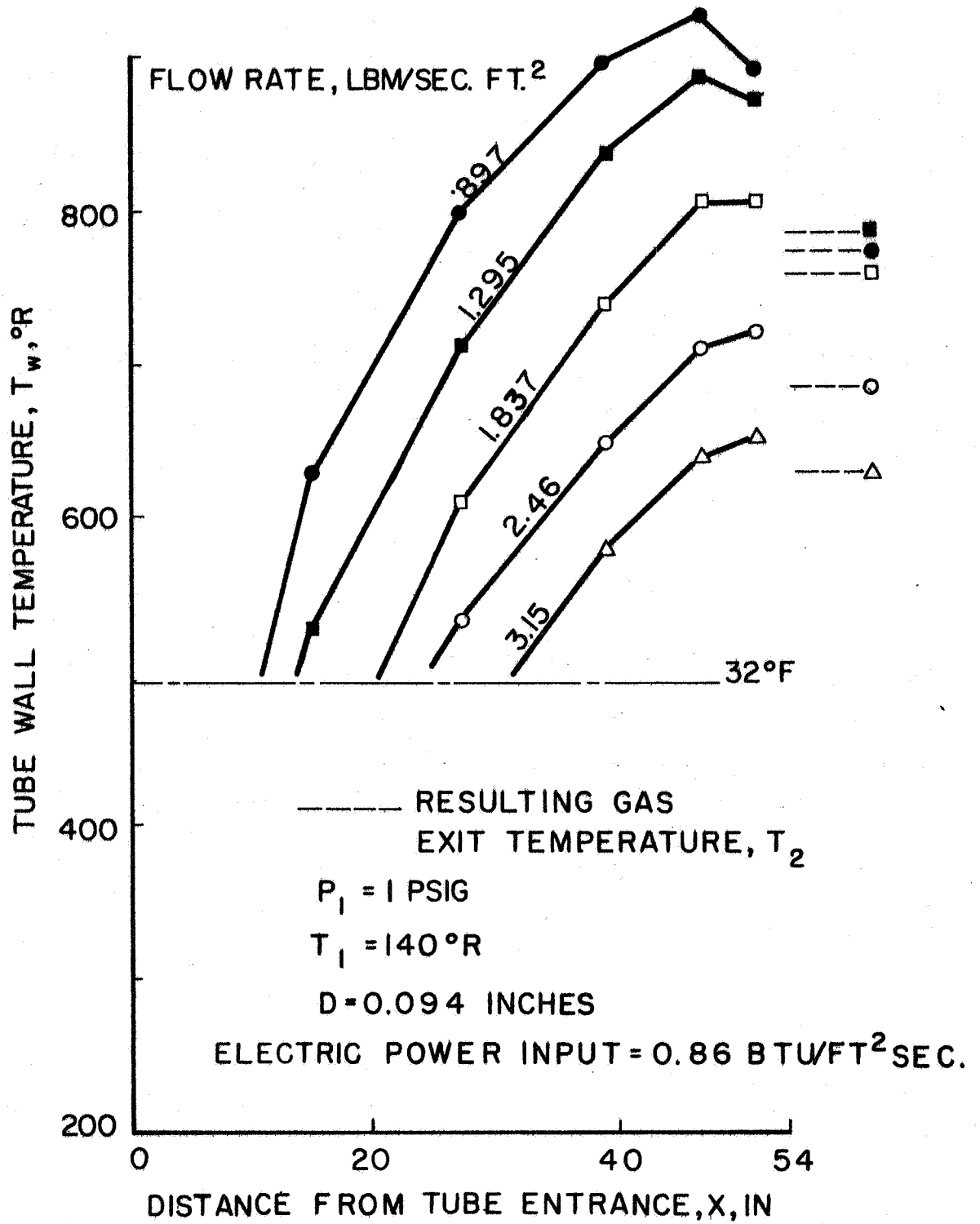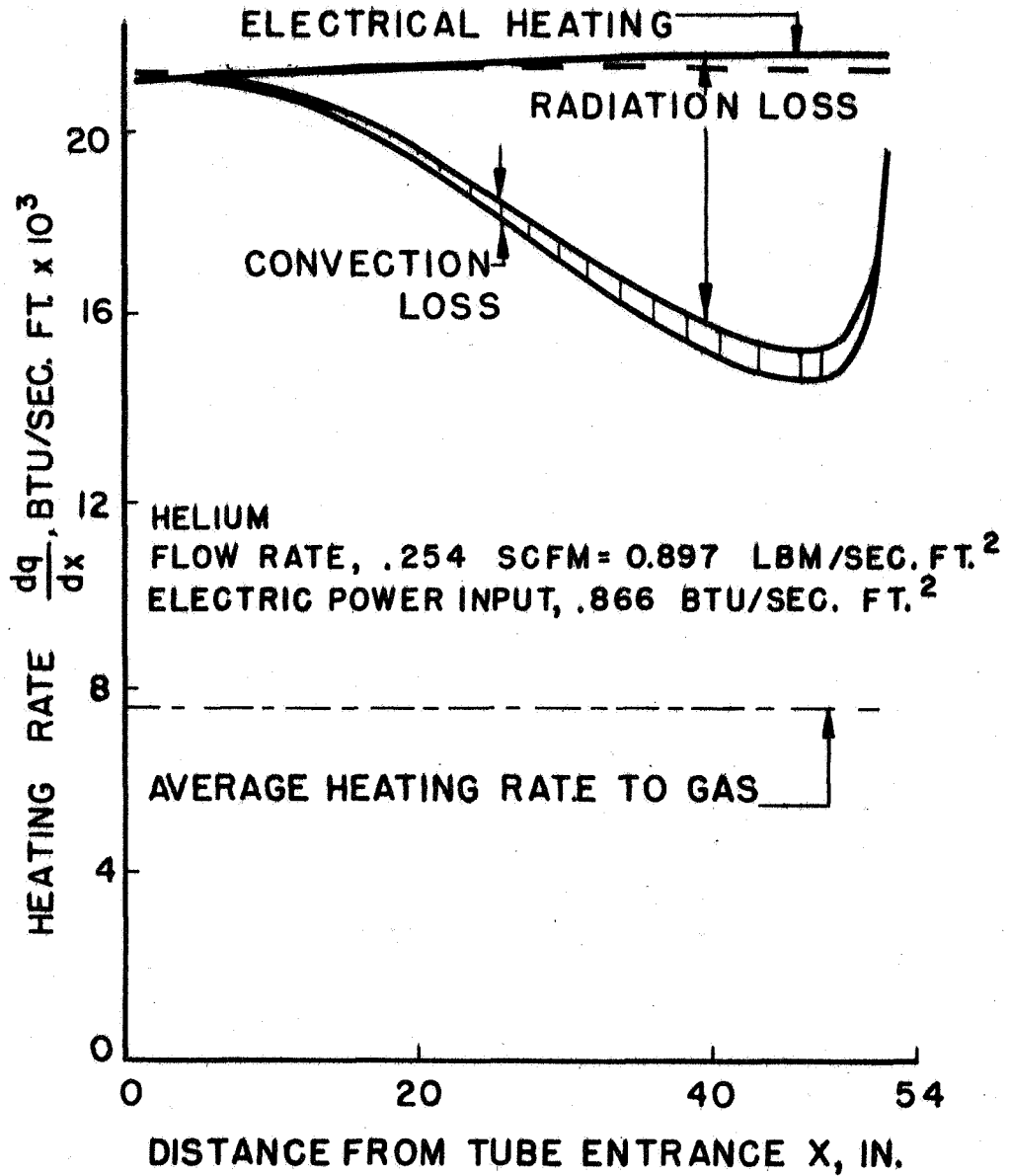
f   Fanning friction factor

g   Gravitational acceleration

G_r Grashof number $\equiv (\frac{g\beta\rho^2}{\mu^2})(\Delta T)(x^3)$

h   Convection heat transfer coefficient

k   Thermal conductivity

L   Tube length

m Density of "reactor core" material

m   Exponent of viscosity variation with temperature $\mu = \mu_o T^m$

M   Mach number

n   Exponent of friction factor variation with Reynolds number $f = \dfrac{f_o}{Re^n}$

Nu   Nusselt number $\equiv \dfrac{hx}{k}$

p,P   Pressure

Pr   Prandtl number

q   Heating rate per unit mass of fluid

Q   Heating rate per unit inside surface area of tube

$\overline{Q}$ Average heating rate per unit inside surface area of tube

R   Gas constant

Re   Reynolds number

r_h Hydraulic radius ($= \frac{D}{4}$ for round tubes)

s   Entropy

T   Absolute Temperature

t   Time

u   Velocity in x direction

w   Mass flow rate

x   Distance along the tube

β Thermal expansion coefficient

ε Emissivity

ρ Density

σ Stefan–Boltzmann constant

τ Temperature ratio T_{out}/T_{in}

SUBSCRIPTS

f   Evaluated at film conditions

b   Evaluated at bulk conditions

i   Initial value

w   Evaluated at wall

o   Initial constant

1   Inlet

2   Outlet

APPENDIX B

HARRY'S SOLUTION OF STEADY-STATE OPERATING CURVES

1. Numerical Technique

The assumption of one dimensional flow is made; the equations solved are the following: (List of symbols is given in Appendix A)

Continuity (B1)

$$\frac{d}{dx}(\rho A u) = 0$$

Momentum (B2)

$$\frac{1}{\rho} \frac{dp}{dx} + u \frac{du}{dx} + \frac{f}{r_h} \frac{u^2}{2} = 0$$

Energy (B3)

$$\frac{q}{u} + \frac{f}{r_h} \frac{u^2}{2} = T \frac{ds}{dx}$$

q , the power per unit mass of fluid is assumed balanced by Q , the power per unit of surface area since only the steady case is being considered at this time.

$$Q \pi D x = q \rho A x$$

or $$Q = \rho q r_h$$

Also, $$Q = h(T_w - T_b)$$

where, for laminar flow,

$$h = (\frac{k}{D})(1.75)(\frac{wC_p}{kx})^{1/3}$$

and, for turbulent flow,

$$h = \frac{k}{D}(.023)Re^{.8}Pr^{.333}[1 + (\frac{4r_h}{x})^{.7}]$$

with all terms evaluated at film conditions.

An assumed laminar-turbulent hysteresis transition is used. The Fanning friction factor f is found from $f = 16/Re$ for laminar flow and from

$$\frac{1}{\sqrt{f\frac{T_f}{T_b}}} = 4 \log(Re \frac{\rho_f}{\rho_b} \sqrt{f\frac{T_f}{T_b}}) - .4 , \qquad (B4)$$

a modified form of the Karman-Nikuradse equation, for turbulent flow.

2. Closed-Form Approximation

The assumptions used by Harry for this analysis are the following:

      a.   Constant tube cross section

      b.   Perfect gas relationship

      c.   Very low Mach numbers

d. Friction Factor approximated by

$$f = f_o/Re^n$$

e. Viscosity approximated by

$$\mu = \mu_o T^m$$

f. Constant heat distribution along the tube;

$$Q(x) = Q_o$$

The results of integration can be written:

$$p_1 \Delta p = RT_1 \left(\frac{W}{A}\right)^2 \left(\frac{Q_o x}{r_h\left(\frac{W}{A}\right)C_p T_1} + \frac{f_o \mu_1^n r_h\left(\frac{W}{A}\right)C_p T_1}{\left(4r_h \frac{W}{A}\right)^n 2Q_o r_h (mn+2)}\right.$$

$$\left.\left\{\left[1 + \frac{Q_o x}{r_h\left(\frac{W}{A}\right)C_p T_1}\right]^{mn+2} - 1\right\}\right) \tag{B5}$$

The slope of the curve of $p_1 \Delta p$ vs. $\left(\frac{W}{A}\right)$ is found by

differentiating equation B5 with respect to (w/A). Using
the fact that

$$wC_p \Delta T = Q_o x \pi D ,$$

this gives

$$\frac{\partial(p_1 \Delta p)}{\partial(\frac{w}{A})}\bigg|_{Q_0} = RT_1\{\frac{Q_0 L}{r_h C_p T_1} +$$

$$\frac{f_1 L w}{2 r_h A}[\frac{3-n}{mn+2}\ \frac{\tau^{mn+2}-1}{\tau-1} - \tau^{mn+1}]\} \hspace{1cm} \text{(B6)}$$

If equation B5 is rewritten as

$$\Delta p = \frac{R}{p_1}(\frac{w}{A})^2[T_2 - T_1] +$$

$$\frac{R}{p_1}(\frac{w}{A})^2[\frac{f_1 L}{2 r_h}\ \frac{T_1}{mn}\ \frac{\tau^{mn+2}-1}{\tau-1}]$$

it is more easily seen that the first term represents momentum

pressure drop; the second term represents friction pressure drop.

As flow decreases, temperature and the laminar friction factor

increase; the second term predominates and pressure drop begins to

increase giving rise to the left branch of the curve[*]

---

[*]The fact that turbulent flow is always associated with a
positive slope is a consequence of the fact that the friction factor
f in turbulent flow is a much weaker function of viscosity (and
hence, of temperature) than it is in laminar flow:

$$f_{LAM} = \frac{16}{Re}$$

$$f_{TURB} \approx \frac{.046}{Re^{.2}} \hspace{1cm} \text{(From Ref. 2)}$$

3. Correlation Parameters

The momentum pressure drop term of equation B5 is very small at low flow rates. By neglecting this term, substituting in perfect gas and other suitable relations, the non-dimensional equation

$$\psi = fcn(Re_1, \phi)$$

is obtained. Coefficients are evaluated at inlet conditions and are defined as:

$$\psi \equiv \frac{D}{L}\left(\frac{Dp_1}{C_1\mu_1}\right)^2 \frac{\Delta p}{p_1}$$

$$Re_1 \equiv \frac{D\,\rho_1 u_1}{\mu_1}$$

$$\phi \equiv \frac{Q_o L}{\mu_1 C_{p_1} T_1}$$

These coefficients, when evaluated from data calculated from Harry's numerical analysis (Section 1.), produce a fairly smooth curve as seen in Figure 4.

APPENDIX C

CALCULATION OF HEAT LOSSES

1. Convection Loss from the Test Section

In order to calculate the convection loss at the worst conditions, the highest wall temperature profile recorded was used. This corresponded to a flow rate of .254 scfm as seen in Figure 15. A tank pressure of close to .5 mmHg was obtainable with the vacuum pump used, however this pressure increased during operation due to a small leak somewhere in the line. For convection calculations, a tank pressure of 10 mmHg was used. This should give an idea of the largest loss likely to be encountered in these experiments.

Since free convection transfer is proportional to the square root of pressure[12], calculation was carried through for atmospheric conditions and then found for the reduced pressure.

The equation used for the free convection coefficient was (from Ref. 13):

$$\overline{Nu} = .555(GrPr)^{1/4}$$

for low values of Grashof number Gr. The heat transfer was calculated for a series of 3" and 6" intervals along the tube.

$$\Delta T = \overline{T}_w - T_{AIR}$$

where $\overline{T}_W = \dfrac{T_1 + T_2}{2}$ for each interval.

Gas properties for each interval were evaluated at film conditions from Ref 13

with $T_f = \dfrac{\overline{T}_W + T_{AIR}}{2}$

Heat transfer to that portion of the tube which was below air temperature was neglected. Taking account of the heating of this cold section would have reduced the final value of convection heat loss.

The result for these "worst" conditions was that the convection heat loss would be about 1.3% of the heating rate of .85 Btu/sec ft^2 going into the tube.

2. Radiation Loss from the Test Section

$$q_{NET} = \sigma(T_W^4 - T_{TANK}^4)A_W F$$

For a small gray body in black surroundings, $A_W F \rightarrow A_W \varepsilon$ where ε is the emissivity of the test section and A_W is its area.[13] The emissivity of the tanks is about .96 (for rough steel plate[13]) and so is considered balck.

The emissivity of the Nichrome test section was taken as .6[14]. Calculation of radiated heat per unit area was performed at various

points along the tube. The heat radiated per unit length was then plotted; graphical integration of this curve gave the total radiation loss. Radiation transfer to the cold section of the tube was neglected.

In Figure 16, results of the radiation and convection loss calculations are plotted as a function of distance from tube entrance for the case of $w = .254$ scfm. The electrical heating curve is not horizontal due to variation of resistivity along the tube. This variation is small, as expected. The upper horizontal line is the value of $\frac{dQ}{dx}$ corresponding to a nominal heating rate of $.866$ Btu/sec ft^2 which would occur if there were no variations or losses. The lower horizontal line is the value of dQ/dx corresponding to the average heating rate to the gas.

REFERENCES

1. Spence, Roderick W.; and Durham, Franklin P.: The Los Alamos Nuclear-Rocket Program. Astronautics and Aeronautics, June, 1965.

2. Bussard, R. W.; and DeLauer, R. D.: Fundamentals of Nuclear Flight. McGraw-Hill Book Company, 1965.

3. Harry, David P., III: A Steady-State Analysis of the "Laminar-Instability" Problem Due to Heating Para-Hydrogen in Long, Slender Tubes, NASA TN D-2084, 1964.

4. Turney, George E.; and Smith, John M.: Steady-State Investigation of Laminar-Flow Instability Problem Resulting from Relatively Large Increases in Temperature of Normal Hydrogen Gas Flowing in Small Diameter Heated Tube. NASA TN D-3347, 1966.

5. Guevara, F. A.; M^{C}Inteer, B. B.; Potter, R. M.: Temperature-Flow Stability Experiments. Los Alamos Scientific Laboratory. LAMS-2934, 1963.

6. Reshotko, Eli; An Analysis of the "Laminar Instability" Problem in Heated Reactor Passages. AIAA Preprint 66-588, June 1966.

7. Taylor, Maynard F.; Experimental Local Heat-Transfer and Average Friction Data for Hydrogen and Helium Flowing in a Tube at Surface Temperatures up to 5600°R . NASA TN D-2280.

8. Tables of the Thermal Properties of Gases. Circular 564. US Department of Commerce. National Bureau of Standards.

9. Reactor Handbook; Volume I, Materials C. R. Tipton Jr., Ed. Interscience Publishers, Inc., 1960.

10. Taylor, Maynard F.; and Kirchgessner, Thomas A.: Measurements of Heat Transfer and Friction Coefficients for Helium Flowing in a Tube at Surface Temperatures up to 5900°R NASA TN D-133.

11. Technical Catalog NCR-58, Driver-Harris Company
    Harrison, New Jersey.

12. Sulliven, L. B.; Truettner, W. I.; Natural Convection
    Heat Transfer from a Heated Cylinder in Air at
    Sub-atmosheric Pressures. ASHRAE Journal 4:54-9
    April '62.

13. Kreith, F.; Principles of Heat Transfer. International
    Text Book Company.

14. McAdams, W. H.; Heat Transmission 3rd Ed. (New York,
    McGraw-Hill Book Company, Inc., 1954).